Supplement of Atmos. Chem. Phys., 17, 7481–7493, 2017
https://doi.org/10.5194/acp-17-7481-2017-supplement

Atmospheric Chemistry and Physics
Open Access
EGU

Supplement of

Size-resolved chemical composition, effective density, and optical properties of biomass burning particles

J. Zhai et al.

Correspondence to: Xin Yang (yangxin@fudan.edu.cn)

Supplementary Materials

Table S1. Peak values and R squares of the average density distribution of 50, 100, 200, and 400 nm particles at 20 °C (room temperature), 150 °C, and 300 °C. Eff_1 and Eff_2 are the peak values of the effective density modes in Fig. 2. R^2 is the square of the correlation coefficient using Gaussian model fitting.

	50 nm			100 nm			200 nm			400 nm		
	Eff_1	Eff_2	R^2	Eff_1	Eff_2	R^2	Eff_1	Eff_2	R^2	Eff_1	Eff_2	R^2
20°C	1.167	\	0.980	0.933	1.454	0.979	0.939	1.519	0.9697	1.344	1.917	0.966
150 °C	0.972	1.642	0.951	0.981	1.691	0.932	0.984	1.746	0.949	1.094	1.798	0.911
300 °C	0.976	1.756	0.851	0.994	1.851	0.864	1.030	1.857	0.850	1.157	2.051	0.779

Table S2. Single scattering albedo (SSA) at wavelengths of 530 nm and 450 nm and Ångström absorption exponent (AAE) of total biomass burning particles at 20 °C (room temperature), 150 °C, and 300 °C.

Temperature	SSA		AAE
	450 nm	530 nm	
Room temperature (20 °C)	0.750	0.897	6.230±0.160
150 °C	0.533	0.723	5.047±0.246
300 °C	0.469	0.560	2.229±0.292

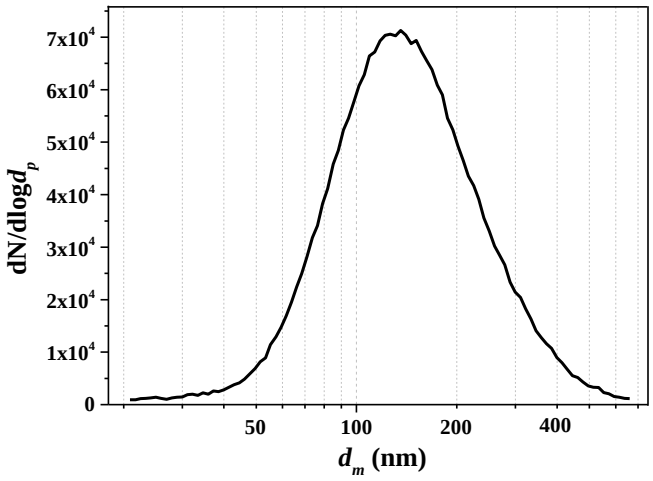

Figure S1. Average number size distribution of biomass burning particles detected by the Scanning Mobility Particle Sizer (SMPS).

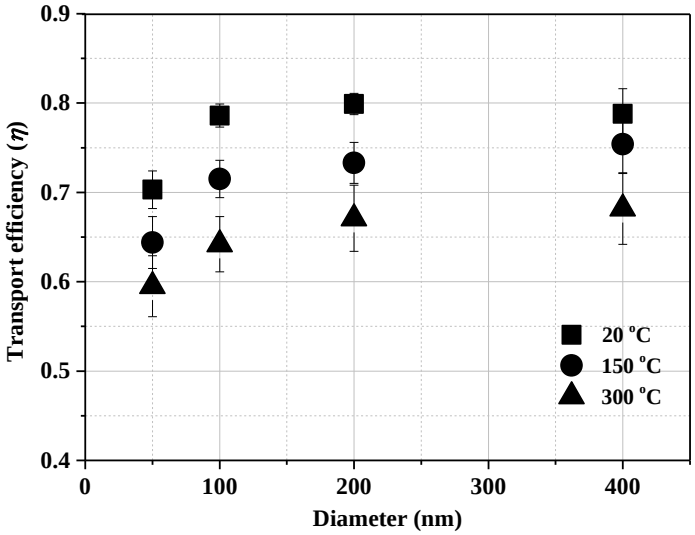

Figure S2. Transport efficiency of NaCl in the thermodenuder as a function of particle diameter and heating temperature.

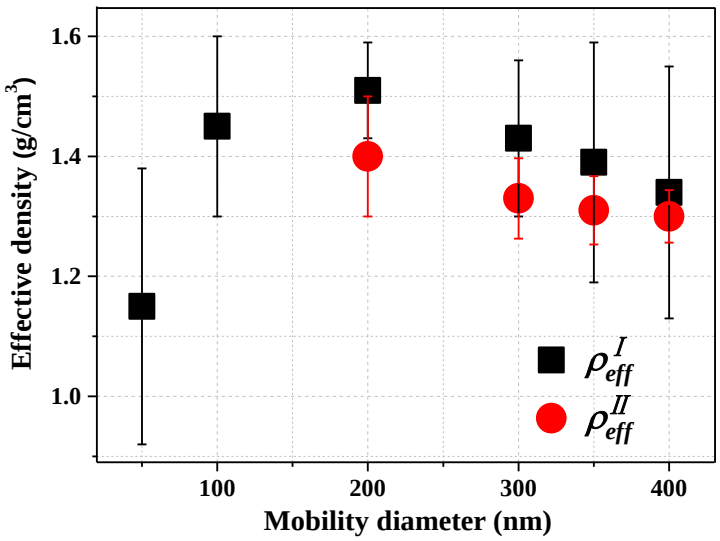

Figure S3. Size-resolved effective density of biomass burning particles determined by two methods. ρ_{eff}^{I} is the effective density obtained from mobility and mass measurements (based on the DMA-APM-CPC system) while ρ_{eff}^{II} is obtained from mobility and aerodynamic measurements (DMA-SPAMS system). The effective density of each size is the average peak value of the dominant mode from different scans. Error bars represent the standard deviations of the five replicate test results.

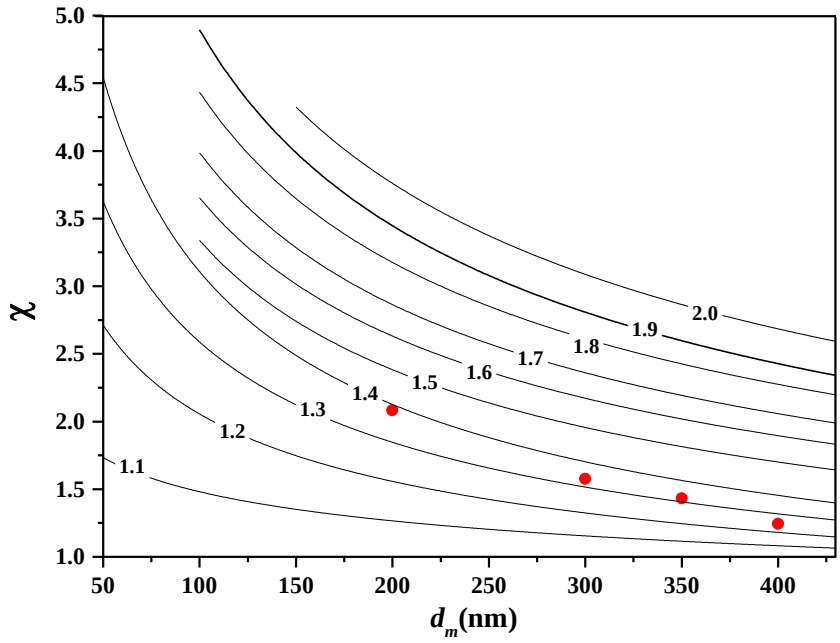

Figure S4. Contour plot of the ratio of the estimated particle mass (m_p) to the exact m_p. The estimated m_p was obtain by replacing ρ_{eff}^{I} with calculated ρ_{eff}^{II} in Equation (2). The ratios of the estimated m_p by replacing ρ_{eff}^{I} with exact ρ_{eff}^{II} in Equation (2) to the exact m_p was shown as well (red dots).

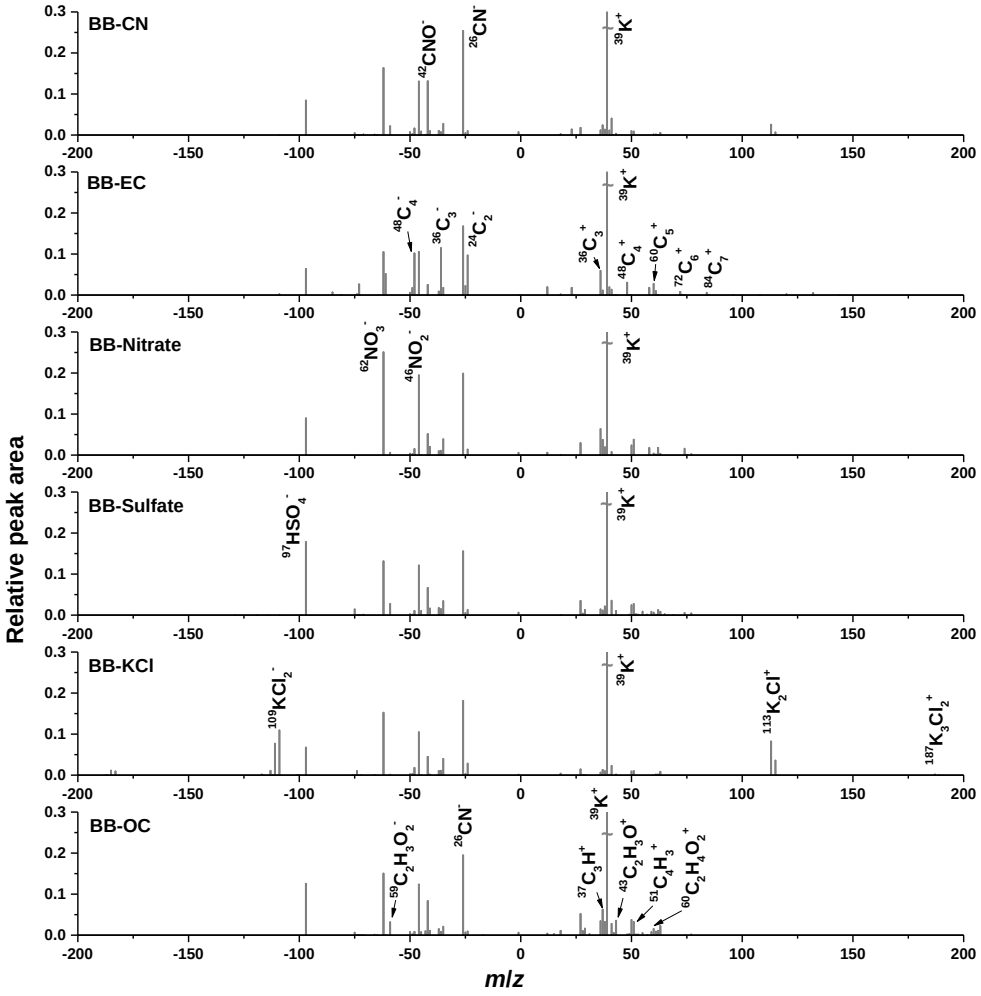

Figure S5. Average mass spectra of 6 particle types classified from biomass burning particles.